Liquid Crystals
Publication details, including instructions for authors and subscription information:
http://www.informaworld.com/smpp/title~content=t713926090

Threshold voltage for purely flexoelectric deformations of conducting homeotropic nematic layers

Grzegorz Derfel[a]; Mariola Buczkowska[a]
[a] Institute of Physics, Technical University of Łódź, 90-924 Łódź, Poland

To cite this Article Derfel, Grzegorz and Buczkowska, Mariola(2007) 'Threshold voltage for purely flexoelectric deformations of conducting homeotropic nematic layers', Liquid Crystals, 34: 1, 113 — 125
To link to this Article: DOI: 10.1080/02678290601061546
URL: http://dx.doi.org/10.1080/02678290601061546

Liquid Crystals, Vol. 34, No. 1, January 2007, 113–125

Threshold voltage for purely flexoelectric deformations of conducting homeotropic nematic layers

GRZEGORZ DERFEL* and MARIOLA BUCZKOWSKA
Institute of Physics, Technical University of Łódź, ul. Wólczańska 219, 90-924 Łódź, Poland

(*Received 5 June 2006; accepted 25 August 2006*)

Elastic deformations induced by an electric field in homeotropic nematic layers with finite anchoring energy were studied numerically. A nematic material possessing flexoelectric properties and characterized by a positive dielectric anisotropy was considered. The ionic space charge and the ion transport across the layer were taken into account. The director orientation, the electric field strength and the ion concentrations were calculated as functions of the coordinate normal to the layer. The calculations show that the electric field distribution, which determines the form of the deformations, is influenced by the ionic current and therefore depends on the ionic content and on the properties of the electrodes. Several types of deformations were distinguished. When the electrode contacts are well conducting or when the ionic content is low, the threshold voltage is very close to the value U_f valid for an insulating nematic. When the electrodes are poorly conducting or blocking at high ion concentration, the threshold voltage decreases much below U_f. At moderate ion concentrations, i.e. between 10^{19} and $10^{20}\,m^{-3}$, two different behaviours were found depending on the sign of the sum of flexoelectric coefficients $e_{11}+e_{33}$. In the case of $e_{11}+e_{33}<0$, the threshold voltage decreases with the ionic content; in the case of $e_{11}+e_{33}>0$, the deformations occur in two separate voltage regimes. They arise above a certain threshold voltage, disappear at some higher voltage and reappear at an even higher threshold.

1. Introduction

Electric field induced deformations of nematic liquid crystal layers may arise due to dielectric anisotropy or to flexoelectric properties of the liquid crystalline material. However, if the nematic with positive dielectric anisotropy, $\Delta\varepsilon>0$, is confined between parallel electrode plates and if its alignment is perfectly homeotropic, the dielectric properties give rise to a torque which quenches the deformations. (The same concerns the perfectly planar layer if $\Delta\varepsilon<0$.) Therefore the arising deformations have purely flexoelectric nature. They may be initiated by the surface flexoelectric torques (if the anchoring strength is sufficiently low) or by the bulk flexoelectric torque (if electric field gradients arise due to the ionic space charge).

A weakly anchored homeotropic layer of nematic liquid crystal with a positive dielectric anisotropy and flexoelectric properties determined by the negative sum of flexoelectric coefficients $e_{11}+e_{33}<0$ was considered in an earlier paper [1]. Ion transport across the layer was excluded since perfectly blocking electrodes were assumed. In the present paper, we report the results of numerical calculations for a similar system with the same set of parameters as was used in [1], however we take into account the flow of the ionic current. Our aim is to determine the role of ionic transport in flexoelectric deformations. Such a role was also studied in [2] and [3], for somewhat different systems in which the negative dielectric anisotropy favoured deformations.

In the case of a perfectly insulating nematic, flexoelectric deformations of the layer are possible if the inequality

$$(e_{11}+e_{33})^2 > k_{33}\varepsilon_0\Delta\varepsilon \tag{1}$$

is satisfied [4]. They have threshold character with the threshold voltage U_f given by the formula

$$\coth\left(\pi\frac{U_f}{U_c}\right) = \frac{Wd}{2\pi k_{33}}\frac{U_c}{U_f}\left\{\left(\frac{\pi k_{33}}{Wd}\frac{U_f}{U_c}\right)^2\left[\left(\frac{U_c(e_{11}+e_{33})}{\pi k_{33}}\right)^2-1\right]-1\right\} \tag{2}$$

where $U_c=\pi[k_{33}/(\varepsilon_0|\Delta\varepsilon|)]^{\frac{1}{2}}$, W is the anchoring strength, k_{33} is the bend elastic constant and d is the thickness of the layer. Close to the threshold the director profiles described by the angle between the distorted director

*Corresponding author. Email: gderfel@p.lodz.pl

Liquid Crystals
ISSN 0267-8292 print/ISSN 1366-5855 online © 2007 Taylor & Francis
http://www.tandf.co.uk/journals
DOI: 10.1080/02678290601061546

and its initial orientation, $\theta(z)$ (where z is the coordinate perpendicular to the layer), are expressed by the combination of $\sinh(\pi\zeta U/U_c)$ and $\cosh(\pi\zeta U/U_c)$.

The ions that are usually present in the liquid crystal material have an important influence on the electric field distribution within the sample and therefore affect the field-induced deformations. This influence was demonstrated by our earlier calculations [1] performed for a layer confined between perfectly blocking electrodes, which excluded current flow in the external circuit. The threshold voltage decreased significantly when the ion concentration was sufficiently high. This decrease was attributed to the strong and highly inhomogeneous electric field which arose in the vicinity of the electrodes under these circumstances.

In a more realistic case considered in the present paper, we admit the flow of the ionic current, based on the weak electrolyte model for a nematic in the bulk [5]. We consider various properties of the electrode contacts, from strongly blocking to well conducting. For this purpose, we apply the same simplified model for electrical phenomena taking place at the nematic–electrode interface that was adopted earlier [2, 3].

The form of deformations is determined by the electric field distribution, which is influenced by the ionic space charge. The spatial distribution of ions is in turn dependent on the properties of the electrodes and on the electrical properties of the nematic, in particular on the ionic mobilities. Therefore the transport of ions plays a crucial role in the deformations. Our aim is to study the formation of deformations at various ionic contents and for various types of electrode contact.

The calculations allowed us to determine director profiles, electric field distributions and ion concentrations within the layer as well as the threshold voltages U_T; the main results are as follows. When the electrodes are well conducting or when the ionic content is low, the threshold is practically independent of ion concentration. In the case of a negative sum of the flexoelectric coefficients, the threshold voltage decreases strongly with the average ion concentration when the electrodes have pronounced blocking character, whereas it remains practically constant and close to U_f when the electrode–nematic contacts are well conducting. In the case of a positive sum of flexoelectric coefficients, an unusual behaviour was predicted. When the electrodes are poorly conducting and the ion concentration ranges between 10^{19} and $10^{20}\,m^{-3}$, deformations are induced in two separate voltage regimes: the deformations arise at a certain low threshold voltage, disappear at some higher voltage and reappear at even higher threshold.

In § 2, the parameters of the system under consideration are given. In § 3, the results of calculations are presented separately for $e_{11}+e_{33}<0$ and for $e_{11}+e_{33}>0$; § 4 is devoted to their discussion and briefly summarizes the results of the present work and of [2] and [3].

2. Method: geometry and parameters

The material and layer parameters were similar to those used in our previous papers [1–3]. A nematic liquid crystal layer of thickness $d=20\,\mu m$ was confined between two infinite plates parallel to the xy-plane of the Cartesian coordinate system. They were positioned at $z=\pm d/2$, and played the role of electrodes. A voltage U was applied between them; the lower electrode ($z=-d/2$) was earthed. Homeotropic alignment was assumed. The anchoring strength W was identical on both surfaces and was equal to $10^{-5}\,J\,m^{-2}$. The director $\mathbf{n}$ was parallel to the xz-plane, its orientation described by the angle $\theta(z)$, measured between $\mathbf{n}$ and the z-axis. The model substance was characterized by the elastic constants $k_{11}=6.2\times10^{-12}\,N$ and $k_{33}=8.6\times10^{-12}\,N$. Positive dielectric anisotropy $\Delta\varepsilon=2$ was adopted with the dielectric constant components $\varepsilon_\parallel=7.4$ and $\varepsilon_\perp=5.4$. The flexoelectric properties were expressed by the sum of flexoelectric coefficients $e_{11}+e_{33}$ (separate values of e_{11} and e_{33} are not essential in the geometry considered [4]). Their absolute magnitude was equal to $40\times10^{-12}\,C\,m^{-1}$. Both signs of $e_{11}+e_{33}$ were taken into account.

The transport of ions under the action of an electric field was characterized by their mobility and diffusion coefficients. It was assumed that the mobility of cations was much smaller than that of anions. The values used in calculations corresponded to typical results of mobility measurements in various liquid crystals: $\mu_\parallel{}^-=1.5\times10^{-9}$, $\mu_\perp{}^-=1\times10^{-9}$, $\mu_\parallel{}^+=1.5\times10^{-10}$, $\mu_\perp{}^+=1\times10^{-10}\,m^2\,V^{-1}\,s^{-1}$, and reflected a typical anisotropy of mobility, i.e. $\mu_\parallel^\pm/\mu_\perp^\pm=1.5$. The Einstein relation was assumed for the diffusion constants: $D_{\parallel,\perp}^\pm=(k_BT/q)\mu_{\parallel,\perp}^\pm$, where q denotes the absolute value of the ionic charge, k_B is the Boltzmann constant and T is the absolute temperature. The weak electrolyte model [5] was adopted in which the ion concentration was determined from the generation and recombination constants. The generation constant β was varied between 10^{18} and $10^{24}\,m^{-3}\,s^{-1}$ in order to control the ion content. The recombination constant α was equal to $3.8\times10^{-18}\,m^3\,s^{-1}$. The resulting average ion concentration N_{av}, defined as

$$N_{av}=\frac{1}{2d}\left\{\int_{-d/2}^{d/2}[N^+(z)+N^-(z)]\,dz\right\} \qquad (3)$$

where $N^{\pm}(z)$ denote the concentrations of ions of corresponding sign, ranged from 10^{17} to $5\times10^{20}\,m^{-3}$.

The electrode properties were described in terms of our model which has already been presented in detail [2, 3]. It is based on a general concept of electrode reactions, which are governed by the energy barriers φ arising between the liquid crystal and the electrodes. They are due to differences between the work function of the electrode and affinity of the electron to the molecule, as well as between the ionization energy of the molecule and the work function of the electrode. The height of a barrier φ plays the role of activation energy of a corresponding electrode process and determines its rate.

The electrode contacts were characterized by the rates of generation and neutralization of the ions at the electrodes, and determined by a single parameter K_r. In order to illustrate possible essentially distinct behaviours of the layer, the calculations were carried out with several different values of K_r: 10^{-7}, 10^{-6}, 10^{-5}, 10^{-4} and $10^{-3}\,m\,s^{-1}$. The lowest value corresponds to strongly blocking contacts whereas the highest value denotes the well conducting case.

The conductivity of an electrode can be defined as $S=j/E(\pm1/2)$, where the electric current density j is chosen as a measure of the charge exchange on the electrode. In general, the conductivity S is not constant for a given electrode. The S values are of the order 10^{-11}–$10^{-7}\,\Omega^{-1}\,m^{-1}$, depending on the parameters β_0 and K_r. The calculated electric current density is not proportional to the electric field strength at the electrode; proportionality occurs only in the case of well conducting contacts. The conductivity of the electrode increases with the parameter K_r in a nonlinear way (approximately $S\sim K_r^{\eta}$, where $\eta\approx0.2$–0.5) however there is no exact correlation between both quantities. The K_r value is identical for both anode and cathode, whereas the surface electric field strengths may differ (due to asymmetry caused by the difference between mobilities of anions and cations), $E(-1/2)\neq E(+1/2)$, thus giving different values of S. For this reasons, our model is not equivalent to the approach which uses the concept of conductivity of electrodes, and we have therefore not introduced it in this paper.

The problem is considered to be one-dimensional. The system is described by a set of ten equations [2,3] which consists of a torque equation for the bulk, two torque equations for the boundaries, an electrostatic equation, two equations of continuity of anion and cation fluxes in the bulk, and four equations describing the boundary conditions for ion transfer across the electrode contacts.

The numerical solutions yielded the director configurations, described by the angle $\theta(\zeta)$, the electric field strength distributions $E(\zeta)$ and the ion concentrations $N^{\pm}(\zeta)$ for various voltages and generation constants β (where $\zeta=z/d$ is the reduced coordinate). The results allowed us to determine the threshold voltages U_T for the deformations with an accuracy of 0.01 V.

3. Results

All the deformations revealed by the calculated $\theta(\zeta)$ functions have threshold character. The threshold voltage U_T depends on the average ion concentration as well as on the properties of the electrodes. The deformations occurring at various average ion concentrations and various K_r values have different forms; the corresponding director profiles result from the distributions of the electric field which are related to the distributions of ions.

In most cases, ions are separated by an external voltage and accumulate in the vicinity of the electrodes of opposite sign. The layer becomes electrically charged as a whole, since the total number of negative ions is lower than the number of positive ions. (The lacking negative charge is placed in the external circuit.) The difference is *c.* 25% at low N_{av} but decreases below 1% at high concentrations. It is the stronger, the less conducting are the electrodes. The effect is evidently connected with the difference between mobilities of anions and cations; the number of faster ions is smaller than that of the slower. Additional calculations (partially presented in [3]) show that when $\mu^+=\mu^-$, the numbers of cations and of anions are equal to N_0 and the net charge vanishes. By contrast, the net charge becomes larger when μ^+ is decreased with respect to fixed μ^-. The ion concentrations in the layer are governed by all the equations mentioned in §2. They describe complex phenomena including dissociation, recombination, transport in the electric field, diffusion, electrode processes, as well as the electric field distribution. A qualitative explanation of the considered effect on the basis of these equations appears to be rather difficult.

3.1. *Negative sum of flexoelectric coefficients*

3.1.1. Threshold voltage. The results are shown in figure 1, where $U_T(N_{av})$ is plotted for five values of K_r and for the perfectly blocking case. For very low ion concentrations ($10^{17}\,m^{-3}$), the threshold is practically equal to the value $U_f=7.23$ V obtained from the formula valid for an insulating nematic, equation (2). The properties of the electrode contacts are negligible in this case. Their role becomes important if the ion concentration increases.

In the case of well conducting electrodes, $K_r=10^{-3}\,m\,s^{-1}$, the threshold voltage weakly depends

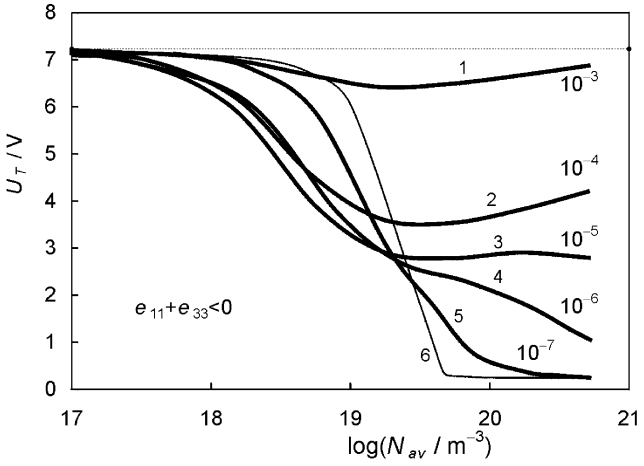

Figure 1. Threshold voltage U_T as a function of average ion concentration N_{av}, for five values of K_r indicated at each curve (in m s^{-1}) and for perfectly blocking electrodes (thin line); $e_{11}+e_{33}<0$. The dashed line represents the threshold $U_f=7.23$ V.

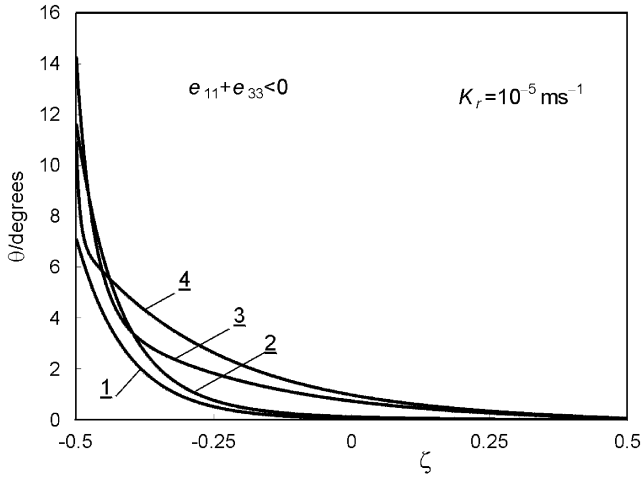

Figure 2. Director orientation angle θ as a function of the reduced coordinate ζ for $U=U_T+0.1$ V and $K_r=10^{-5}$ m s^{-1}; $e_{11}+e_{33}<0$. Average ion concentrations (in m^{-3}) and voltages are as follows. 1: $N_{av}=1.25\times10^{18}$, $U=6.20$; 2: $N_{av}=5.74\times10^{18}$, $U=3.97$; 3: $N_{av}=5.44\times10^{19}$, $U=2.88$; 4: $N_{av}=5.28\times10^{20}$, $U=2.89$.

on N_{av} (curve 1). It is close to U_f at low ionic contents, reaches a minimum value of 6.4 V at moderate $N_{av}=10^{19}$ m^{-3} and approaches the value U_f at high concentrations.

If the electrode contacts are poorly conducting, the threshold voltage decreases with N_{av}. The lower the rate of the electrode processes K_r, the stronger is this reduction, (curves 2–5). The non-monotonic $U_T(N_{av})$ dependence can be seen in curves 2 and 3. The lowest threshold is obtained for the high ion concentration, $N_{av}\cong5\times10^{20}$ m^{-3}, and strongly blocking electrodes, $K_r=10^{-7}$ m s^{-1} (curve 5). Its value, $U_T=0.24$ V, is 30 times lower than U_f. This behaviour is very similar to that found for perfectly blocking electrodes (curve 6), and corresponds to the results presented in [1].

3.1.2. Director distributions. Three types of director distribution can be distinguished. They are shown in figures 2 and 3 by means of $\theta(\zeta)$ profiles plotted for voltages exceeding the threshold by 0.1 V.

Type 1. A distribution with director tilt limited to the neighbourhood of the negative electrode. The director orientation changes monotonically from maximum deviation at $\zeta=-1/2$ to zero at $\zeta=1/2$. Distortion of this form occurs at any type of electrode contact if the ion concentration is only low or moderate. Examples are given for $K_r=10^{-5}$ m s^{-1} in figure 2 (curves 1 and 2) and for $K_r=10^{-7}$ m s^{-1} in figure 3 (curves 1 and 2). Similar distributions were obtained for $K_r=10^{-3}$ and 10^{-4} m s^{-1}. They were also observed in the case of perfectly blocking electrodes [1].

Type 2. A distribution with rapid decrease of director deviation in a thin sub-electrode region at the negative electrode (figure 2; curve 4). In the rest of the layer the orientation changes monotonically as in the previous case. This form of distortion appears for poorly conducting contacts and high ion concentrations.

Type 3. A distribution with rapid changes of orientation at the electrodes and linear variation of the angle θ with ζ (figure 3, curves 3, 4 and 5). This type of deformation is seen for strongly blocking contacts,

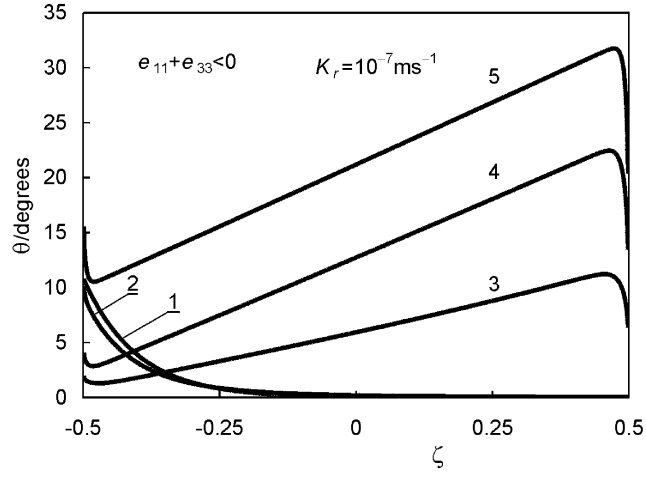

Figure 3. Director orientation angle θ as a function of the reduced coordinate ζ for $U=U_T+0.1$ V and $K_r=10^{-7}$ m s^{-1}; $e_{11}+e_{33}<0$. Average ion concentrations (in m^{-3}) and voltages are as follows. 1: $N_{av}=7.2\times10^{17}$, $U=7.19$; 2: $N_{av}=1.85\times10^{19}$, $U=3.14$; 3: $N_{av}=7.90\times10^{19}$, $U=0.85$; 4: $N_{av}=1.92\times10^{20}$, $U=0.46$; 5: $N_{av}=5.53\times10^{20}$, $U=0.34$.

$K_r=10^{-7}\,m\,s^{-1}$, if the ion concentration is sufficiently high ($N_{av}>10^{20}\,m^{-3}$); it starts at a very low threshold voltage. It was observed in a nematic with negative dielectric anisotropy confined between strongly blocking electrodes [2] as well as in the case of perfectly blocking contacts for both signs of $\Delta\varepsilon$ [1]. These observations indicate that the sign of $\Delta\varepsilon$ is unimportant for type 3 distribution.

3.1.3. Ion concentration and electric field strength. *Poorly conducting electrodes*. The sub-electrode space charge density is particularly remarkable when the electrodes are poorly conducting, $K_r<10^{-4}\,m\,s^{-1}$, and if the average ion concentration is high. Representative examples are given in figure 4 for $K_r=10^{-5}\,m\,s^{-1}$. Figure 5 shows corresponding distributions of the electric field. If the ion concentration is sufficiently low, $N_{av}<10^{18}\,m^{-3}$, the field is practically uniform and equal to U/d (curve 1). At moderate ion concentrations, $N_{av}\approx 5\times10^{18}$–$10^{19}\,m^{-3}$, an electric field gradient appears in the bulk and spreads over the prevailing part of the layer (curve 2). When the ion concentration is high, the electric field strength in the bulk decreases much below U/d, while strong sub-surface electric fields together with high gradients arise at the electrodes (curves 3 and 4).

Strongly blocking electrodes. The effects mentioned above are more pronounced if the electrodes are strongly blocking, which is shown in figure 6 by the functions $|E(\zeta)|$ plotted for $K_r=10^{-7}\,m\,s^{-1}$. The concentrations at the surfaces are nearly two orders of magnitude higher than in the bulk. As a result, a high and non-uniform electric field arises in the vicinity of the electrodes. The electric field in the bulk is significantly reduced to about $0.005U/d$ due to the sub-surface sheets of the space charges (figure 6, curve 4).

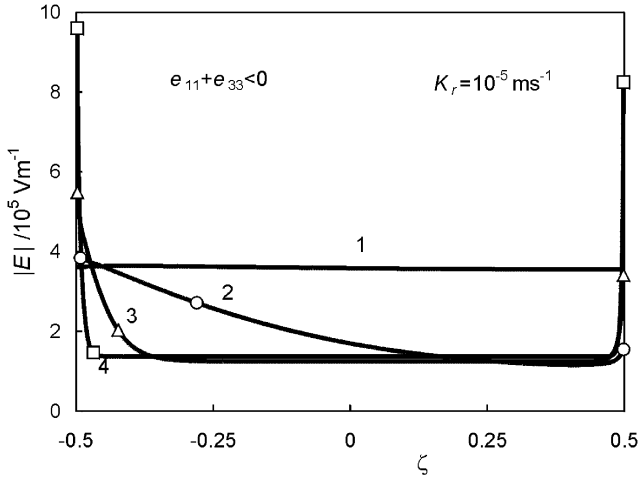

Figure 5. Electric field strength $|E|$ as a function of the reduced coordinate ζ for $K_r=10^{-5}\,m\,s^{-1}$; $e_{11}+e_{33}<0$. Average ion concentrations (in m^{-3}), voltages and Debye lengths (in μm) are as follows. 1: $N_{av}=1.67\times10^{17}$, $U=7.17$, $L_D=4.72=0.236d$; 2: $N_{av}=5.74\times10^{18}$, $U=3.97$, $L_D=0.80=0.04d$; 3: $N_{av}=5.44\times10^{19}$, $U=2.88$, $L_D=0.26=0.013d$; 4: $N_{av}=5.28\times10^{20}$, $U=2.89$, $L_D=0.084=0.0042d$. Circles (2), triangles (3) and squares (4) indicate values of $|E(\pm1/2)|$.

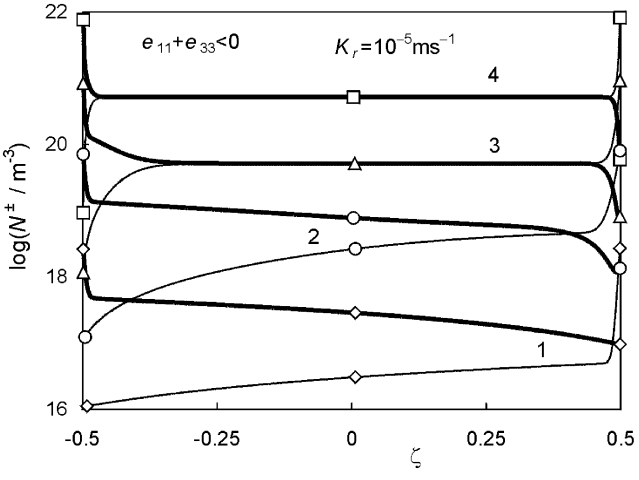

Figure 4. Ion concentration as a function of the reduced coordinate ζ for $K_r=10^{-5}\,m\,s^{-1}$; thick lines denote positive ions, thin lines denote negative ions; $e_{11}+e_{33}<0$. Average ion concentrations (in m^{-3}) and voltages are as follows. 1: $N_{av}=1.67\times10^{17}$, $U=7.17$; 2: $N_{av}=5.74\times10^{18}$, $U=3.97$; 3: $N_{av}=5.44\times10^{19}$, $U=2.88$; 4: $N_{av}=5.28\times10^{20}$, $U=2.89$. Diamonds (1), circles (2), triangles (3) and squares (4) indicate concentration values at $\zeta=\pm1/2$.

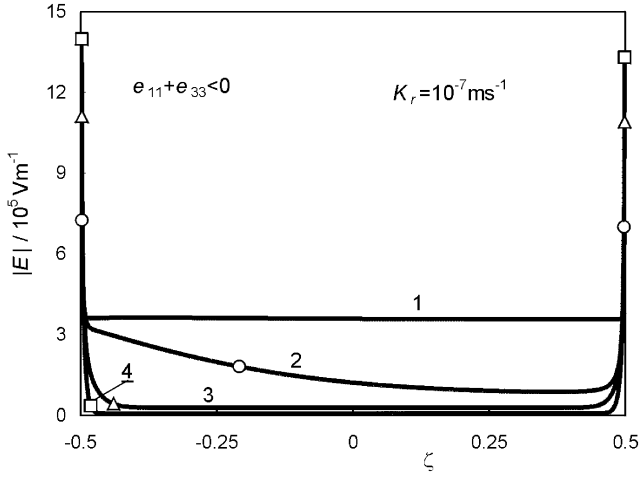

Figure 6. Electric field strength $|E|$ as a function of the reduced coordinate ζ for $K_r=10^{-7}\,m\,s^{-1}$; $e_{11}+e_{33}<0$. Average ion concentrations (in m^{-3}), voltages and Debye lengths (in μm) are as follows. 1: $N_{av}=7.2\times10^{17}$, $U=7.18$, $L_D=2.3=0.135d$; 2: $N_{av}=1.85\times10^{19}$, $U=3.14$; $L_D=0.448=0.0224d$; 3: $N_{av}=7.90\times10^{19}$, $U=0.85$, $L_D=0.22=0.011d$; 4: $N_{av}=5.53\times10^{20}$, $U=0.34$, $L_D=0.082=0.0041d$. Circles (2), triangles (3) and squares (4) indicate values of $|E(\pm1/2)|$.

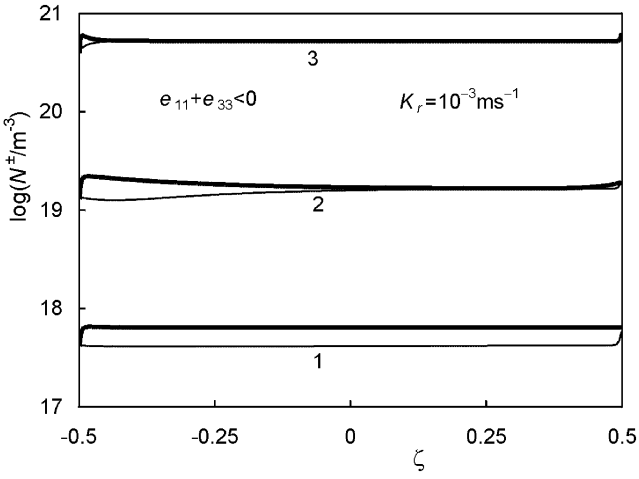

Figure 7. Ion concentrations as functions of the reduced coordinate ζ for $K_r=10^{-3}\,m\,s^{-1}$; $e_{11}+e_{33}<0$. Thick lines denote positive ions, thin lines denote negative ions. Average ion concentrations (in m^{-3}) and voltages are as follows. 1: $N_{av}=5.27\times10^{17}$, $U=7.23$; 2: $N_{av}=1.66\times10^{19}$, $U=6.52$; 3: $N_{av}=5.27\times10^{20}$, $U=6.98$.

Well conducting electrodes. In the case of well conducting contacts, $K_r=10^{-3}\,m\,s^{-1}$, the concentration of positive ions is slightly enhanced at the positive electrode and slightly lowered at the negative electrode (figure 7). The electric field is uniform when the ionic content is low (figure 8, curve 1). In the case of high ion concentration, the field at the negative electrode is somewhat higher than in the bulk, (curves 2 and 3).

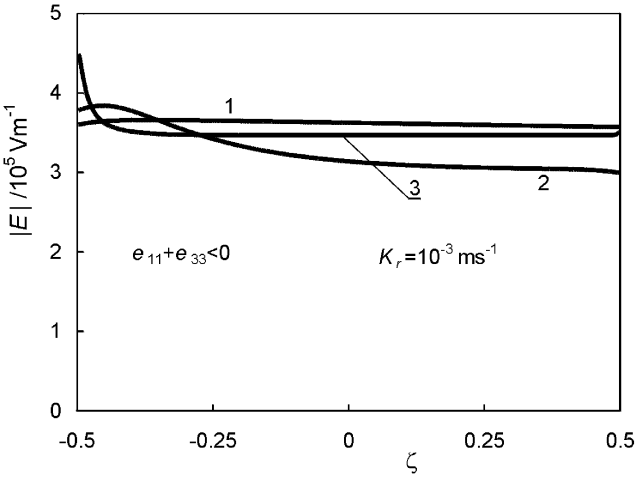

Figure 8. Electric field strength $|E|$ as a function of the reduced coordinate ζ for $K_r=10^{-3}\,m\,s^{-1}$; $e_{11}+e_{33}<0$. Average ion concentrations (in m^{-3}) and voltages are as follows. 1: $N_{av}=5.27\times10^{17}$, $U=7.23$; 2: $N_{av}=1.66\times10^{19}$, $U=6.52$; 3: $N_{av}=5.27\times10^{20}$, $U=6.98$.

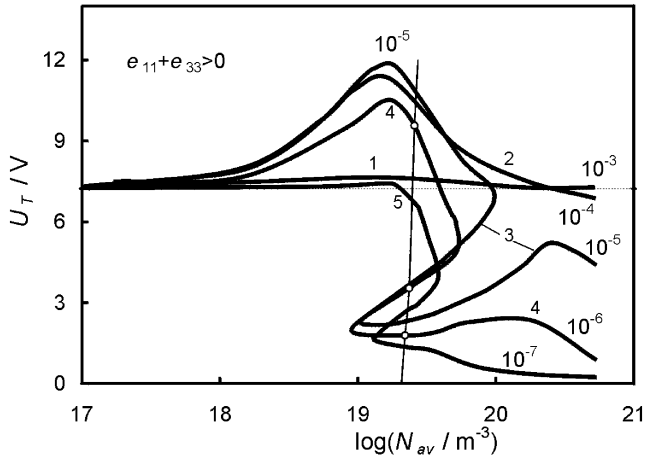

Figure 9. Threshold voltage as a function of average ion concentration N_{av}, for six values of K_r indicated at each curve (in $m\,s^{-1}$); $e_{11}+e_{33}>0$. The dashed line represents the threshold for a perfectly insulating nematic, $U_f=7.23$ V. The thin oblique line corresponds to data presented in figure 2 for $K_r=10^{-6}\,m\,s^{-1}$; circles indicate the threshold voltages for a nematic with $\beta_0=10^{21}\,m^{-3}\,s^{-1}$.

3.2. *Positive sum of flexoelectric coefficients*

3.2.1. Threshold voltage. The results are shown in figure 9, where $U_T(N_{av})$ is plotted for five values of K_r. At very low ion concentrations ($10^{17}\,m^{-3}$), the threshold is practically equal to the value $U_f=7.23$ V. As previously, the properties of the electrode contacts are negligible. They become important at higher ion concentration.

In the case of well conducting electrodes ($K_r=10^{-3}\,m\,s^{-1}$), the threshold voltage weakly depends on N_{av} and also remains close to U_f (curve 1). Three distinct phenomena can be noted:

(a) The threshold voltage reaches a maximum at $N_{av}\approx10^{19}\,m^{-3}$. The maximum reaches *c*. 12 V for $K_r=10^{-4}\,m\,s^{-1}$, whereas it only slightly exceeds U_f for $K_r=10^{-7}$ and $10^{-3}\,m\,s^{-1}$.

(b) The threshold voltage decreases significantly at high ion concentrations, $N_{av}\geqslant10^{20}\,m^{-3}$. Its value depends on the electrode properties. It is close to U_f for $K_r\geqslant10^{-4}\,m\,s^{-1}$ (curve 2) and decreases to several tenths of a volt for strongly blocking contacts, $K_r=10^{-7}\,m\,s^{-1}$ (curve 5).

(c) At ion concentrations between 10^{19} and $10^{20}\,m^{-3}$ and for $K_r\leqslant10^{-5}\,m\,s^{-1}$, the deformations are induced in two separate voltage ranges (curves 4, 5, 6). The lower range has a finite width, the upper spreads above a critical voltage. Such behaviour is illustrated in figure 10, where the optical phase difference between the ordinary and extraordinary rays, $\Delta\Phi$ (calculated for $\lambda=632.8$ nm), is used as a quantity indicating the

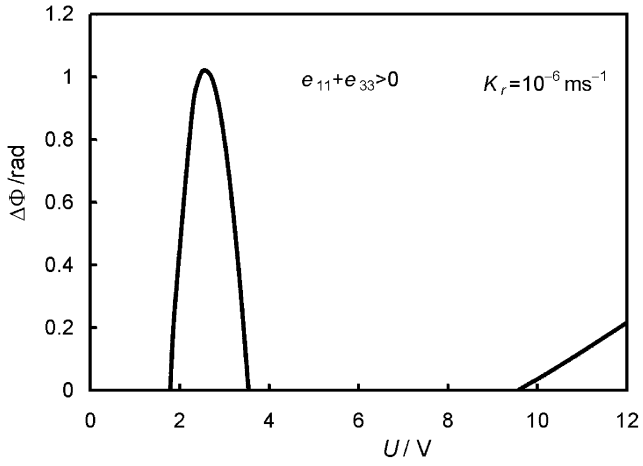

Figure 10. Optical phase retardation $\Delta\Phi$ as a function of the bias voltage U; $\beta_0=10^{21}\,m^{-3}\,s^{-1}$; $K_r=10^{-6}\,m\,s^{-1}$; $e_{11}+e_{33}>0$.

occurrence of deformation. It is plotted as a function of applied voltage for $\beta_0=10^{21}\,m^{-3}\,s^{-1}$ and $K_r=10^{-6}\,m\,s^{-1}$. (The data correspond to the thin oblique line plotted in figure 9.) It is evident that the deformations appear at a certain threshold voltage, disappear at some higher voltage and reappear at an upper threshold (1.79, 3.54 and 9.57 V, respectively). The deformations occurring in these two regions have different forms described in the next section.

3.2.2. Director distributions. One can distinguish four types of deformation. They are exemplified in figure 11

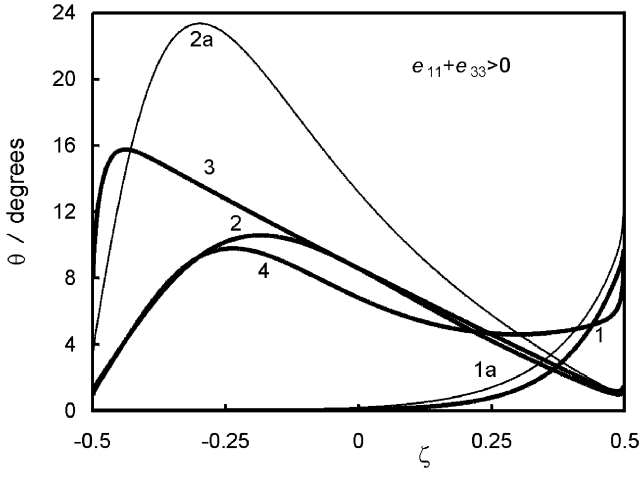

Figure 11. Director orientation angle θ as a function of the reduced coordinate ζ for $K_r=10^{-7}\,m\,s^{-1}$ (thick lines) and $K_r=10^{-6}\,m\,s^{-1}$ (thin lines). Average ion concentrations (in m^{-3}) and voltages are as follows. 1: $N_{av}=5.16\times10^{18}$, $U=7.41$; 1a: $N_{av}=2.60\times10^{19}$, $U=10$; 2: $N_{av}=2.31\times10^{19}$, $U=2.65$; 2a: $N_{av}=2.27\times10^{19}$, $U=2.5$; 3: $N_{av}=7.57\times10^{19}$, $U=0.72$; 4: $N_{av}=4.11\times10^{19}$, $U=3.6$.

by means of $\theta(\zeta)$ profiles and have the following main features:

Type 4. Deformation is limited to the positive half of the layer. The angle θ increases monotonically with ζ to the largest value at $\zeta=1/2$, (figure 11, curves 1 and 1a). Deformations of type 4 arise at any ion concentration if $K_r\geqslant10^{-4}\,m\,s^{-1}$. Type 4 occurs also if two voltage regimes exist; in such a case it arises above the upper threshold. This type of director distribution is analogous to the type 1 described above for $e_{11}+e_{33}<0$.

Type 5. Director distortion reaches a maximum in the negative half of the layer (figure 11, curves 2 and 2a). Almost linear variation with the z-coordinate takes place in the positive half. Type 5 arises in the lower voltage range.

Type 6. Director deviation from the layer normal increases rapidly in the close vicinity of the negative electrode and reaches a maximum. In the remaining part of the layer, the angle θ decreases linearly with ζ to a very low value at $\zeta=1/2$ (figure 11, curve 3). Type 6 appears at high ion concentrations above a strongly reduced threshold in the case of strongly blocking electrodes. It corresponds to type 3 described in § 3.1.2 for $e_{11}+e_{33}<0$ and was observed also in [3].

Type 7. The director distribution is intermediate between types 4 and 5. The maximum distortion in the left half of the layer is lower and the deformation at $\zeta=1/2$ is stronger than in the case of type 5 (figure 11, curve 4). Type 7 can be found above the upper threshold when the gap between the two voltage ranges is very narrow, or at the ion concentration for which the two ranges merge.

3.2.3. Electric field strength. In this section, the electric field strength distributions corresponding to the director profiles mentioned above are described. They are plotted in figure 12 as functions of reduced coordinate ζ for strongly blocking electrodes, i.e. $K_r=10^{-7}\,m\,s^{-1}$. In the case of low ion contents, $N_{av}\approx10^{18}\,m^{-3}$, the electric field strength is almost uniform and close to U_f/d, (curve 1). The subsurface fields are relatively low. The resulting deformation is of type 4. Deformation of type 5, occurring in the lower voltage regime for moderate ion concentrations, $N_{av}\approx10^{19}$–$10^{20}\,m^{-3}$, is induced by the field illustrated by curve 2. The subsurface fields reach much higher values than U_f/d, and large field gradients arise in the subsurface regions. The electric field strength in the bulk also depends on ζ. The bulk field gradient has its origin in the difference between mobilities of positive and negative ions [3] and is practically limited to the negative half of the layer. A qualitatively similar form of the electric field distribution but of larger magnitude (curve 4) corresponds to the deformation of intermediate

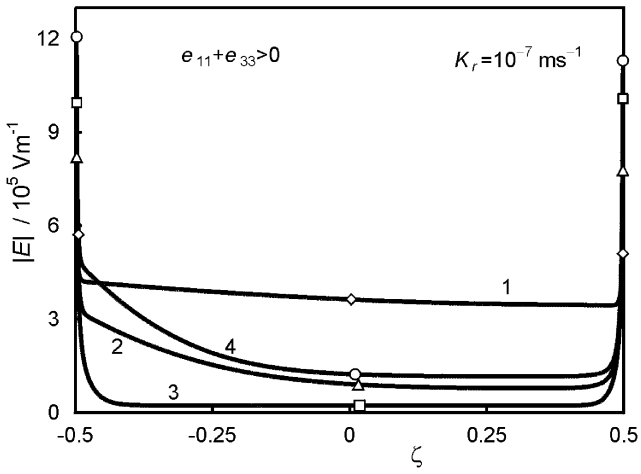

Figure 12. Electric field strength $|E|$ as a function of the reduced coordinate ζ for $K_r=10^{-7}\,\mathrm{m\,s^{-1}}$; $e_{11}+e_{33}>0$. Average ion concentrations (in $\mathrm{m^{-3}}$) and voltages are as follows. 1: $N_{av}=5.16\times10^{18}$, $U=7.41$; 2: $N_{av}=2.31\times10^{19}$, $U=2.65$; 3: $N_{av}=7.57\times10^{19}$, $U=0.72$; 4: $N_{av}=4.11\times10^{19}$, $U=3.6$. Diamonds (1), triangles (2), squares (3) and circles (4) indicate the values of $|E(\pm1/2)|$.

type 7. In the case of high ion concentrations, $N_{av}>10^{20}\,\mathrm{m^{-3}}$, the electric field in the bulk is much lower than U_f/d and practically uniform (curve 3). The subsurface fields are significantly higher. The field gradients are limited to subsurface regions, and such an electric field induces the type 6 deformation.

Figure 13 shows the electric field distribution for four voltage values chosen from the lower voltage regime

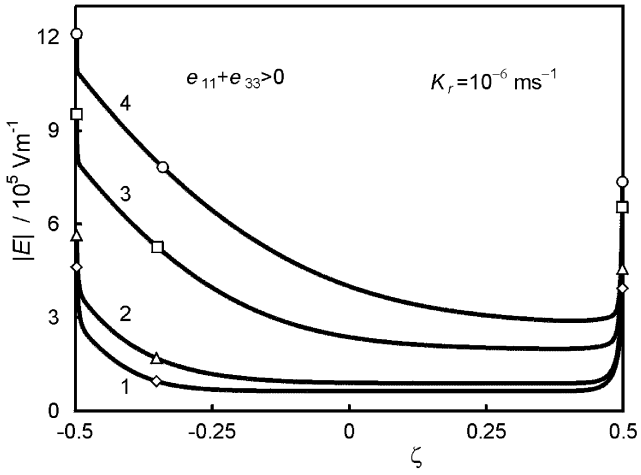

Figure 13. Electric field strength $|E|$ as a function of the reduced coordinate ζ; $\beta_0=10^{21}\,\mathrm{m^{-3}\,s^{-1}}$; $K_r=10^{-6}\,\mathrm{m\,s^{-1}}$; $e_{11}+e_{33}>0$. Average ion concentrations (in $\mathrm{m^{-3}}$) and voltages are as follows. 1: $N_{av}=2.18\times10^{19}$, $U=1.7$ (below the lower threshold); 2: $N_{av}=2.27\times10^{19}$, $U=2.5$ (in the lower voltage regime); 3: $N_{av}=2.49\times10^{19}$, $U=6.5$ (in the gap between voltage regimes); 4: $N_{av}=2.60\times10^{19}$, $U=10$ (in the upper voltage regime). Diamonds (1), triangles (2), squares (3) and circles (4) indicate the values of $|E(+1/2)|$.

(curve 2), from the upper regime (curve 4), from the gap between them (curve 3) and from the range below the lower threshold (curve 1). The data presented by curves 2 and 4 correspond to the deformations shown in figure 11 by means of thin lines 2a and 1a, respectively. All these field distributions have qualitatively the same asymmetrical form typical for moderate ion concentrations. A significant bulk electric field gradient exists in the negative half of the layer. Much greater subsurface gradients are present at both electrodes together with a subsurface field of large strength.

4. Discussion

The behaviour of the system under consideration can be qualitatively interpreted by analysis of the flexoelectric and dielectric torques exerted on the director. They are included in the Euler–Lagrange equation which determines the equilibrium state in the bulk:

$$\frac{1}{2}(k_b-1)\sin 2\theta\left(\frac{d\theta}{d\zeta}\right)^2-\left(\sin^2\theta+k_b\cos^2\theta\right)\frac{d^2\theta}{d\zeta^2}+\frac{1}{2}\frac{\varepsilon_0\Delta\varepsilon}{k_{11}}\sin 2\theta\left(\frac{dV}{d\zeta}\right)^2+\frac{1}{2}\frac{e_{11}+e_{33}}{k_{11}}\sin 2\theta\left(\frac{d^2V}{d\zeta^2}\right)=0 \tag{4}$$

where $k_b=k_{33}/k_{11}$, and in the two equations which determine the boundary conditions for $\theta(\zeta)$:

$$\pm\frac{1}{2}\frac{e_{11}+e_{33}}{k_{11}}\sin 2\theta(\pm1/2)\left.\frac{dV}{d\zeta}\right|_{\pm1/2}\mp\left[\sin^2\theta(\pm1/2)+k_b\cos^2\theta(\pm1/2)\right]\left.\frac{d\theta}{d\zeta}\right|_{\pm1/2}-\frac{1}{2}\gamma\sin 2\theta(\pm1/2)=0 \tag{5}$$

for $\zeta=\pm1/2$, where $\gamma=Wd/k_{11}$.

The dielectric torque acts in the bulk of the layer and is always stabilizing. The flexoelectric torque in the bulk of the layer is proportional to the electric field gradient $dE/d\zeta$, i.e. to $d^2V/d\zeta^2$. When the sum $e_{11}+e_{33}$ is negative and only the positive angles $\theta(\zeta)$ occur, this torque is stabilizing if $d^2V/d\zeta^2<0$, whereas it favours the deformation in the opposite case.

The flexoelectric torque at the surfaces is proportional to the electric field strength $E(\pm1/2)$. It may give rise to the deformation if the term $\pm[(e_{11}+e_{33})/(2k_{11})](dV/d\zeta)|_{\pm1/2}$ in equation (5) is positive. If $e_{11}+e_{33}<0$, positive values of $dV/d\zeta$ result in a destabilizing torque at $\zeta=-1/2$ and quench the deformation at $\zeta=+1/2$.

When the sum $e_{11}+e_{33}$ is positive, the reversed relationships are valid. This means that the bulk torque is stabilizing if $d^2V/d\zeta^2>0$, whereas it favours the

deformation in the opposite case. Positive values of $dV/d\zeta$ result in a destabilizing surface torque at $\zeta=+1/2$ and quench the deformation at $\zeta=-1/2$. Schematic diagrams relating the stabilizing and destabilizing actions of the flexoelectric torques to the electric field distribution for the case of $e_{11}+e_{33}>0$ are shown in figure 14.

The magnitudes of each of these five contributions depend on the number of ions and on their spatial distributions $N^{\pm}(\zeta)$, since these quantities determine the electric field strength and its gradient.

The effectiveness of surface torques depends on the electric field strengths at the surfaces. The effectiveness of bulk torques depends not only on their absolute magnitude but also on the thicknesses of the regions in which they act. The qualitative explanation as to why the deformation occurs, or why it does not occur, can be given by analysis of the electric field distribution within the layer which allows the estimate of contributions of the various torques. However such an analysis of the torques can be done only *a posteriori*. The only

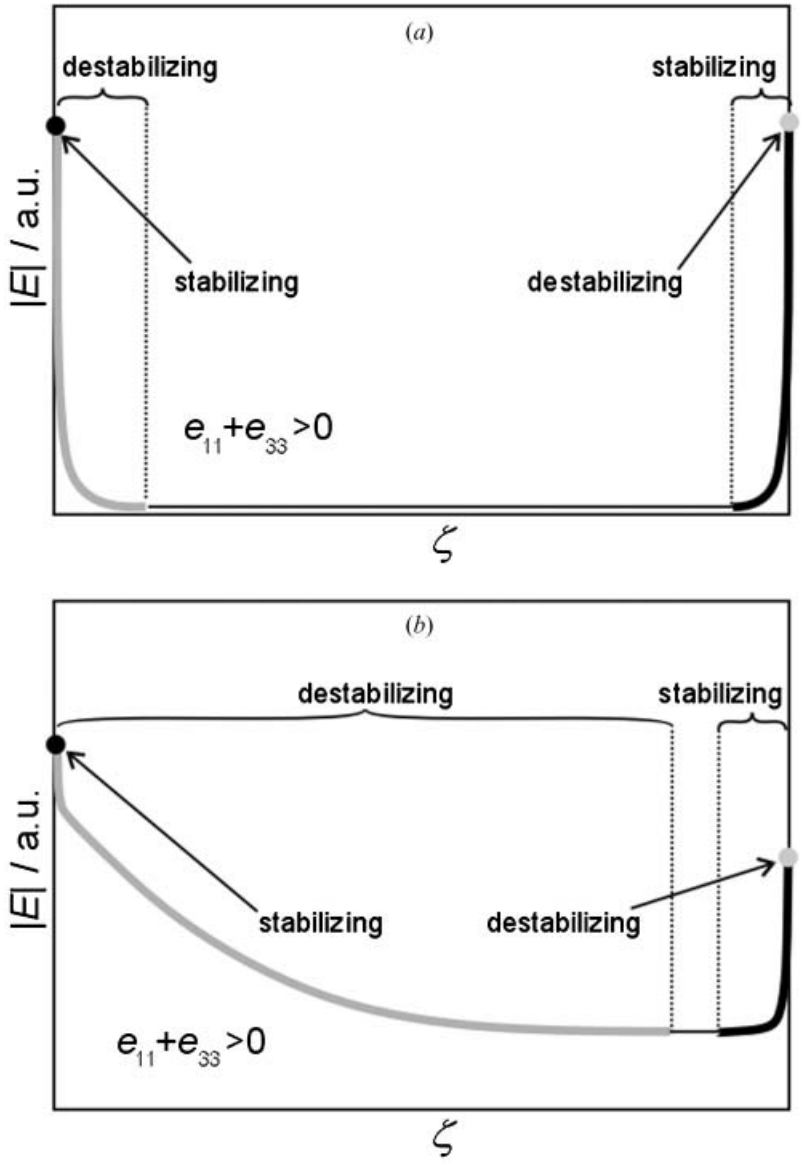

Figure 14. Two examples of the relationship between electric field distribution and flexoelectric torque for $e_{11}+e_{33}>0$: (*a*) high ion concentrations, (*b*) moderate ion concentrations. The electric field distributions corresponding to regions of stabilizing and destabilizing torques in the bulk are marked by thick lines, black and grey respectively. Black and grey circles denote the surface fields inducing the surface stabilizing and destabilizing torques, respectively. Thin lines denote regions where the flexoelectric torques are negligible.

predictive way is the numerical solution of the set of ten equations mentioned in § 2.

In nematic liquid crystals containing ions, the condition (1) is not necessary for the appearance of flexoelectric deformations. Our additional calculations show that the distortions also appear when $(e_{11}+e_{33})^2 < k_{33}\varepsilon_0\Delta\varepsilon$, only if the electrodes are sufficiently poorly conducting and the ion concentration is sufficiently high. The director distributions are of type 1, but the deformations limited to a rather thin region at the negative electrode, where a large electric field creats a suitable destabilizing flexoelectric torque. In the rest of the layer the dielectric torque quenchs any distortions. The corresponding threshold markedly exceeds the U_f value.

The distributions of electric field and of ion concentration reveal the existence of subsurface layers in which these quantities change rapidly. They are particularly pronounced when the electrodes are poorly conducting ($K_r \leqslant 10^{-5}\,m\,s^{-1}$) and when the average ion concentration exceeds $10^{19}\,m^{-3}$. In such cases, the subsurface layers are responsible for a drastic decrease of the electric field strength in the bulk. Since the sublayers are diffused, their thicknesses cannot be determined strictly. The estimated thicknesses are about 0.2 μm; the corresponding Debye screening length, $L_D=(\varepsilon_{\|}\varepsilon_0 k_B T/2q^2N_{av})^{1/2}$, is somewhat smaller than this value when the ion contents is high (e.g. $L_D=0.084\,\mu m$ at $N_{av}=5.3\times10^{20}\,m^{-3}$). It has comparable magnitude in the case of moderate ion concentrations (e.g. $L_D=0.26\,\mu m$ at $N_{av}=5.4\times10^{19}\,m^{-3}$). When the average ion concentration is low, the Debye length is much greater than the thickness of the regions of accumulated charge and is equal to $L_D=4.7\,\mu m$ at $N_{av}=1.7\times10^{17}\,m^{-3}$, for example. In this case, the bulk electric field is practically unscreened. Similar values of L_D and analogous relations with the subsurface layers are obtained for the case of well conducting contacts. Other examples of L_D values are given in the captions to figures 5 and 6. The Debye lengths for the cases presented in figures 12, 13 and 15 range between 0.2 and 0.8 μm according to the moderate ion contents.

4.1. *Director distributions*

4.1.1. Negative sum of flexoelectric coefficients. First, the case of poorly conducting electrodes ($K_r=10^{-7}$–$10^{-5}\,m\,s^{-1}$) is analysed. The highly asymmetric form of the director distribution (type 1) results mainly from the surface flexoelectric torque at the negative electrode, which is destabilizing. The stabilizing dielectric torque in the bulk, as well as the flexoelectric surface torque at $\zeta=+1/2$, quench the deformations in the rest of the layer. The asymmetry is enhanced by the stabilizing

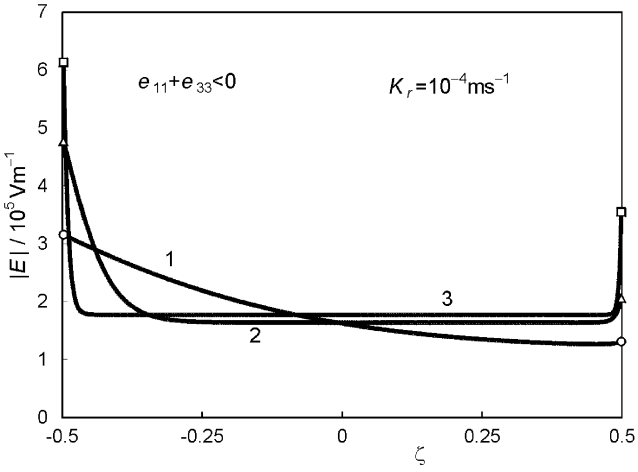

Figure 15. Electric field strength $|E|$ as a function of the reduced coordinate ζ for $U=3.63\,V$ and $K_r=10^{-4}\,m\,s^{-1}$; $e_{11}+e_{33}<0$. Average ion concentrations (in m^{-3}) are as follows. 1: $N_{av}=5.2\times10^{18}$ (no deformation); 2: $N_{av}=5.2\times10^{19}$ (deformation); 3: $N_{av}=5.2\times10^{20}$ (no deformation). Circles (1), triangles (2) and squares (3) indicate the values of $|E(\pm1/2)|$.

flexoelectric torque induced by the electric field gradient $d|E|/d\zeta<0$. At moderate ion concentrations ($N_{av}\sim10^{19}\,m^{-3}$), this gradient spreads over the layer. It is caused by the asymmetric space charge distributions and by the difference in total numbers of positive and negative ions and has its origin in the difference between μ^+ and μ^-.

The type 2 deformation occurring for $K_r=10^{-5}\,m\,s^{-1}$ is due to the particularly large field gradient arising at high ion concentration in the neigbourhood of $\zeta=-1/2$. The resulting flexoelectric torque rapidly damps the deformation in this region. The electric field gradient in the vicinity of the positive electrode yields a torque which is insufficient to overcome the stabilizing actions of the dielectric torque and surface flexoelectric torque.

When the electrodes are strongly blocking ($K_r=10^{-7}\,m\,s^{-1}$) and the ion concentration is high, the gradient in the neighbourhood of $\zeta=1/2$ becomes significantly increased. The resulting destabilizing flexoelectric torque, together with the destabilizing surface torque at $\zeta=-1/2$, give rise to significant deformations, which lead to type 3 director distribution. The linear part of the $\theta(\zeta)$ plot reflects the smooth change of the director orientation unaffected by the electric field and fitted to the orientations imposed by flexoelectric torques in the subelectrode regions. The effect of the dielectric torque is rather small since the bias voltage is low ($U<1\,V$). For this reason, the type 3 distribution was found for both signs of $\Delta\varepsilon$ [1, 2].

The spatial variation of the electric field in the case of well conducting electrodes is weak and the resulting

director distributions are of type 1 due to the destabilizing surface torque at $\zeta=-1/2$.

There are similarities between the results obtained here for $K_r=10^{-7}\,m\,s^{-1}$ and the results reported in [1] where perfectly blocking electrodes were assumed. The profiles presented in figures 2 and 3 are qualitatively the same as in figures 7 and 8 of [1]. Some differences may be due to the processes of generation and recombination of ions which are taken into account here and were ignored previously. These phenomena influence the ion distributions and therefore affect the electric field distributions.

4.1.2. Positive sum of flexoelectric coefficients. The type 4 director distributions represented by curves 1 and 1a in figure 11 is realized in the almost uniform electric field existing at low ion contents (figure 12, curve 1), as well as in the field with significant gradient arising at moderate ion concentrations (figure 13, curve 3). The form of the director distribution indicates that the deformation is induced by the destabilizing surface torque acting at the boundary plate $\zeta=+1/2$. It arises if the electric field $|E(1/2)|$ reaches a sufficient value at which the surface torque overcomes the stabilizing effect of the dielectric torque. In particular, the destabilizing torque due to the field gradient is overwhelmed by the stabilizing dielectric and surface flexoelectric torques, and thus no distortions arise in the negative half of the layer.

The type 5 deformation, appearing in the lower voltage regime, arises mainly as a result of the destabilizing flexoelectric torque originating from the electric field gradient in the vicinity of the negative electrode.

When the electrodes are strongly blocking ($K_r=10^{-7}\,m\,s^{-1}$) and the ion concentration is high, type 6 director distribution appears. The electric field distribution is almost symmetrical with respect to $\zeta=0$. The effect of the difference between cation and anion mobilities is negligible and does not yield a gradient spreading over the layer. Therefore the deformation mechanism is independent of the sign of the flexoelectric coefficients and results in type 6 for $e_{11}+e_{33}>0$ and type 3 for $e_{11}+e_{33}<0$. Type 6 deformations arise mainly due to the subsurface field gradient in the vicinity of $\zeta=-1/2$ that reaches sufficient magnitude at the very low voltage $U<1\,V$. As the bias voltage is so low, the effect of the dielectric torque is rather small; therefore the dielectric anisotropy sign is also unimportant. For this reason, deformations of this type were observed in our earlier calculations performed for $\Delta\varepsilon<0$ [3].

An intermediate type 7 de formation is a result of the relatively comparable actions of the stabilizing surface torque at $\zeta=-1/2$, destabilizing bulk torque in the negative half of the layer, stabilizing dielectric and flexoelectric torques in the neighbourhood of the positive electrode, and destabilizing surface torque on $\zeta=1/2$.

4.2. *Threshold voltage*

4.2.1. Negative sum of flexoelectric coefficients. For very low ion concentrations ($10^{17}\,m^{-3}$) there is no electric field gradient and the deformation is induced only if the electric field $E(-1/2)$ reaches sufficient strength, thus determining the threshold value close to U_f. The same applies to the case of well conducting electrodes. A shallow minimum of U_T observed for $K_r=10^{-3}\,m\,s^{-1}$ at moderate $N_{av}=10^{19}\,m^{-3}$ may be related to a small gradient $d|E|/d\zeta>0$ seen in figure 8 (curve 2).

The decrease of threshold voltage found for poorly conducting electrode contacts and ion concentrations exceeding *c*. $10^{18}\,m^{-3}$, may be due to the destabilizing high electric field $E(-1/2)$ which becomes stronger when N_{av} is increased and when K_r is lowered. The very low threshold voltage found for high ion concentration and strongly blocking electrodes may be considered to be a result of the simultaneous action of two strongly destabilizing flexoelectric torques: surface torque at $\zeta=-1/2$ and bulk torque in the vicinity of $\zeta=1/2$.

The appearance and decay of deformations following the increase of ionic content from low to high average concentration, which is represented by the non monotonic $U_T(N_{av})$ dependence, can be seen, for example, for $K_r=10^{-4}\,m\,s^{-1}$ and constant voltage, $U=3.63\,V$. This effect can be interpreted by considering the electric field distributions for constant voltage at varying ionic content. In figure 15, we plot the representative field distributions for $U=3.63\,V$ and for three ion concentrations. At low and moderate ion concentrations (e.g. $N_{av}\approx5\times10^{18}\,m^{-3}$, curve 1), the electric field gradient spreads over the layer. The resulting stabilizing bulk flexoelectric torque and the stabilizing dielectric torque prevent a deformation. For higher ion contents ($N_{av}\approx5\times10^{19}\,m^{-3}$, curve 2), the gradient becomes limited to a thin region at the negative electrode due to a significant subsurface charge, and its stabilizing action is less effective. The electric field $E(-1/2)$ is much higher, so the destabilizing surface torque at $\zeta=-1/2$ becomes much stronger than previously. The applied voltage $U=3.63\,V$ is therefore sufficient to induce deformation. However further increase of the ion concentration ($N_{av}\approx5\times10^{20}\,m^{-3}$) leads to enhancement of the electric field strength in the prevailing part of the layer (curve 3). The resulting stabilizing dielectric torque becomes stronger and quenches the deformation.

The purely flexoelectric deformations of a conducting nematic layer with positive dielectric anisotropy can be compared with the case of negative dielectric anisotropy in which the layer is dielectrically unstable [2]. For this purpose we have made additional calculations using the surface anchoring strength value $2\times10^{-5}\,\mathrm{J\,m^{-2}}$, according to [2]. The results were qualitatively the same as described above in § 3.1.1. The corresponding values are about double due to stronger anchoring. The threshold voltage is close to $U_f=14.47\,\mathrm{V}$ at low ion concentration and decreases with increasing N_{av} in the same way as shown in figure 1. This behaviour is different from the case considered in [2] where the electric field gradient spreading over the whole layer gave rise to significant enhancement of U_T much above $U_f=3.53\,\mathrm{V}$. The high value of U_f found in the present case shows that the stabilizing dielectric torque is rather strong. Other stabilizing torques play a minor role. In particular, the stabilizing flexoelectric torque in the bulk due to $e_{11}+e_{33}<0$ does not enhance the threshold above U_f and thus it is much less important than in [2].

4.2.2. Positive sum of flexoelectric coefficients. In the case of low N_{av} or for well conducting electrodes, the threshold remains close to U_f, for the same reasons as mentioned above for $e_{11}+e_{33}<0$.

When the electrodes are strongly blocking ($K_r=10^{-7}\,\mathrm{m\,s^{-1}}$) and the ion concentration is high, the subsurface field gradient in the vicinity of $\zeta=-1/2$ reaches sufficient magnitude at very low voltage. In consequence, the threshold decreases to below 1 V. The very low threshold voltage found for high ion concentration and strongly blocking electrodes may be interpreted in the way analogous to the case of $e_{11}+e_{33}<0$ and explained as a result of the simultaneous action of two strongly destabilizing flexoelectric torques: surface torque at $\zeta=+1/2$ and bulk torque in the vicinity of $\zeta=-1/2$.

In the case of poorly conducting or blocking electrodes and at moderate average ion concentrations, the deformations appear in two voltage regimes. The lower threshold is determined by the voltage at which the destabilizing flexoelectric torque, originating in the electric field gradient in the vicinity of the negative electrode, becomes sufficiently effective, i.e. it reaches sufficient magnitude and range in the layer. (Below the lower threshold, this gradient is limited to too narrow a region and induces no deformation.) With increasing voltage, the dielectric torque, as well as the stabilizing flexoelectric surface torque at the boundary $\zeta=-1/2$, become stronger and lead to decay of the distortion. The deformation reappears when the destabilizing surface torque at the boundary $\zeta=+1/2$ overcomes the stabilizing torques.

At moderate ion concentration, the upper threshold exceeds the U_f value. The deformation arises if the electric field $|E(1/2)|$ reaches a sufficient value at which the surface torque overcomes the stabilizing effect of the dielectric torque. For poorly blocking electrodes, $K_r=10^{-5}\,\mathrm{m\,s^{-1}}$, a relatively high voltage is necessary. For strongly blocking contacts, $K_r=10^{-7}\,\mathrm{m\,s^{-1}}$, a sufficiently field high arises at a lower voltage due to the particularly large charges accumulated at the boundaries. Therefore the maximum threshold occurs for $K_r=10^{-5}\,\mathrm{m\,s^{-1}}$, whereas for $K_r=10^{-7}\,\mathrm{m\,s^{-1}}$ its value is close to U_f.

5. Final remarks

In the present paper, we consider the example of a homeotropic layer filled with a nematic material characterized by positive dielectric anisotropy and both negative and positive sum of the flexoelectric coefficients. In previous papers, we studied the deformations arising in a material with negative dielectric anisotropy for which $e_{11}+e_{33}<0$ [2] and $e_{11}+e_{33}>0$ [3]. (Other parameters, as well as the geometry of the layer under consideration, were identical with the exception of the anchoring strength W which was equal to $2\times10^{-5}\,\mathrm{J\,m^{-2}}$. This difference has no qualitative consequences, which was confirmed by additional calculations.) The main results obtained in the considered cases can be summarized as follows:

(a) *Well conducting electrodes*. In all four cases, the well conducting electrodes assure a practically uniform electric field of strength approximately equal to U_f/d. In consequence, the threshold voltage is almost independent of the ion concentration and remains close to U_f.

(b) *Low ion concentrations*. In all four cases, the threshold voltage U_T is close to the U_f value because of the absence of space charges. The behaviour of the layer is similar to the case of the perfectly insulating nematic.

(c) *High ion concentrations*. In all four cases, the threshold voltage strongly depends on electrode properties. For strongly blocking electrode contacts, U_T decreases to several tenths of a volt, because large space charges are accumulated at the boundaries and induce the deformations at low voltage.

(d) *Moderate ion concentrations*. The main differences between the considered cases take place in the range of moderate ion concentrations. They are most pronounced when the electrode contacts are poorly conducting ($K_r<10^{-4}\,\mathrm{m\,s^{-1}}$).

In the cases of negative dielectric anisotropy, the strongest distortion arises in the central part of the layer as a result of bulk dielectric and flexoelectric torques. The most essential bulk flexoelectric torque is due to the electric field gradient resulting from the difference between anion and cation mobilities, which spreads over almost the entire layer. If $e_{11}+e_{33}<0$, this torque is stabilizing and enhances the threshold voltage U_T above U_f. If $e_{11}+e_{33}>0$, the opposite effect occurs; i.e. U_T is smaller than U_f, since the bulk flexoelectric torque is destabilizing in this case and favours the deformations.

In the cases of positive dielectric anisotropy, the bulk flexoelectric torque due to the field gradient appears to be negligible, probably due to the stabilizing action of the dielectric torque. Nevertheless, the difference between cation and anion mobilities is important, since it causes an asymmetry of the electric field distribution: $|E(-1/2)|$ is usually higher than $|E(1/2)|$. In consequence, the destabilizing surface flexoelectric torque at $\zeta=-1/2$, arising when $e_{11}+e_{33}<0$, becomes sufficient for deformation at a lower voltage than for the analogous surface torque which acts at $\zeta=1/2$ when $e_{11}+e_{33}>0$. This asymmetry leads to a decrease of U_T below the U_f value if $e_{11}+e_{33}<0$, and causes an increase of U_T above U_f if $e_{11}+e_{33}>0$.

If $e_{11}+e_{33}>0$ and $\Delta\varepsilon>0$, there exist two regimes of voltage in which the deformations arise, as described in § 3.2.1.

References

[1] M. Felczak, G. Derfel. *Liq. Cryst.*, **30**, 739 (2003).
[2] G. Derfel, M. Buczkowska. *Liq. Cryst.*, **32**, 1183 (2005).
[3] M. Buczkowska, G. Derfel. *Liq. Cryst*, **32**, 1285 (2005).
[4] A. Derzhanski, A.G. Petrov, M.D. Mitov. *J. Phys. (Paris)*, **39**, 273 (1978).
[5] G. Briere, F. Gaspard, R. Herino. *J. chim. Phys.*, **68**, 845 (1971).